Journal of Solution Chemistry, Vol. 34, No. 1, January 2005 (© 2005)
DOI: 10.1007/s10953-005-2074-z

Isentropic Compressibility, Shear Relaxation Time, and Raman Spectra of Aqueous Calcium Nitrate and Cadmium Nitrate Solutions

Nashiour Rohman,[1] Abdul Wahab,[1] and Sekh Mahiuddin[1,*]

Received June 10, 2004; revised September 8, 2004

Speed of sound, viscosity and Raman spectra of aqueous calcium nitrate and cadmium nitrate solutions were measured as functions of molality and temperature. The isentropic compressibility isotherms for both systems cross over in a narrow molality region. In comparison with $Ca(NO_3)_2$(aq) solutions, $Cd(NO_3)_2$(aq) solutions have lower isentropic compressibilities due to a lower charge to radius ratio. The observed Raman spectral changes in the ν_3 ($\approx$1400 cm^{-1}) and ν_4 ($\approx$700 cm^{-1}) modes with an increase in molality suggest that the symmetry of NO_3^- changes from D_{3h} to C_{2v}, and solvent-separated and/or solvent-shared ion pairs are formed in both systems. The results from plotting electrical conductivity *versus* shear relaxation time also imply that the influence of the solvent-separated and/or solvent-shared ion pairs begins $\approx$2.0 mol-kg^{-1} for these systems. The larger $\Delta\nu$ values for the ν_3 mode for $Cd(NO_3)_2$(aq) solutions indicate stronger solvent-separated and/or solvent-shared ion pairs formation in comparison to $Ca(NO_3)_2$(aq) solutions.

KEY WORDS: Cadmium nitrate; calcium nitrate; electrolyte solution; isentropic compressibility; Raman spectra; shear relaxation time; viscosity.

1. INTRODUCTION

In the studies of the solvation structure and the dynamics of ions, especially in water, investigations have been carried out using different techniques [*e.g.*, X-ray[1,2] and neutron[3,4] diffraction, extended X-ray absorption fine structure[5] (EXAFS), and theoretical approaches (*e.g.*, MC and MD computer simulations[6–12])]. In aqueous solutions, the data generated from these methods provide some conclusive interpretations, but in nonaqueous solutions they are often inconclusive. However, the derived structural parameters such as the primary

[1]Material Science Division, Regional Research Laboratory, Jorhat 785 006, Assam, India; e-mail: mahirrljt@yahoo.com

hydration number and the cation–water distance show large variations[13] that depend on the method employed.

The structural information about Ca^{2+} in solutions is important due to its critical function in living cells[5,14,15] as well as in many industrial processes.[16] However, knowledge of the hydration structure of Ca^{2+} is still ambiguous.[7] The geometry of the primary hydration shell of Ca^{2+} is often found to be irregular due to the flexible nature of the hydration shell. The flexibility of the primary hydration shell is also responsible for the absence of the libration band at $\approx$350 cm^{-1} in the low frequency Raman spectra[17,18] for Ca^{2+}(aq).

The reported hydration numbers for Ca^{2+} from diffraction studies[1,13,19] are in the range of 5–8, but Hewish *et al.*[20] suggested from neutron diffraction studies that the co-ordination number of Ca^{2+} in $Ca(NO_3)_2$(aq) changes from 10 to 6 as the molality is varied from 1 to 4.5 mol-kg^{-1}. From X-ray diffraction studies, Caminiti and Magini[21] showed that the co-ordination number of Ca^{2+} is 9 in a very concentrated aqueous calcium nitrate solution, $[Ca(NO_3)_2 \cdot 3.5H_2O]$, whereas in dilute solutions, $(Ca(NO_3)_2 \cdot xH_2O$; $x = 25$ and 40) it is about five to six.[19] Even though recent theoretical[12] calculations demonstrated that the $[Ca(H_2O)_6]^{2+}$, with a water binding energy of 103.4 kJ-mol^{-1} for introduction of the sixth water molecule in the primary hydration shell, has a higher stability than $[Ca(H_2O)_7]^{2+}$ (binding energy = 73.7 kJ-mol^{-1}) or $[Ca(H_2O)_8]^{2+}$ (binding energy = 36.8 kJ-mol^{-1}), the calculated Ca—O bond distance does not match with the experimental values of 246 pm and 247 pm.[1,7] The authors further suggested that the model calculation does not represent the actual geometry and co-ordination of Ca^{2+} in aqueous solution. However, MD simulations[8,9] imply a much higher hydration number, 9 or 10 for Ca^{2+}. Very recently, a combined study[5] of EXAFS, large-angle X-ray scattering (LAXS), and a MD simulation of aqueous calcium halide solutions established that eight water molecules are asymmetrically distributed at an average Ca^{2+}—O distance of 246 pm.

Carpio *et al.*[22] reported speed of sound measurements for $Ca(NO_3)_2$(aq) solutions at 298.15 K. They described the extent of complexation of ions as deduced from isentropic and excess isentropic compressibilities, and inferred the formation of contact ion pairs due to electrostatic interactions. A number of vibrational spectroscopic studies[17,18,23–27] indicated the formation of solvent-separated and contact ion pairs in $Ca(NO_3)_2$(aq) solutions. A recent X-ray diffraction study[1] suggested increasing amounts of contact ion pairing at subzero temperatures due to the reinforcement of the intrinsic structure of water in concentrated $Ca(NO_3)_2$(aq).

On the other hand, the hydration structure of Cd^{2+} seems to be less well characterized. Bol *et al.*[28] reported the presence of an octahedral hydration structure for Cd^{2+} from an X-ray diffraction study. However, using the same method, Kuznetsov *et al.*[29] asserted that the hydration structure of Cd^{2+} changes from tetrahedral to octahedral on increasing the solute molality from 1.388 to 2.220 mol-kg^{-1}. From a Raman spectral investigation, Kanno[30] concluded that

such a transition in the hydration number for Cd^{2+} does not take place, but rather Cd^{2+} remains hexaco-ordinated in $Cd(NO_3)_2$(aq) solutions. Valeev *et al.*[31] reported tetrahedral co-ordination for Cd^{2+} with two water molecules and two nitrate ions for highly concentrated solutions. Both X-ray[31,32] and Raman spectral studies[26,32,33] indicated the presence of a contact ion pair, $[Cd(H_2O)_5ONO_2]^+$, in $Cd(NO_3)_2$(aq) solutions.

The isentropic compressibility of an electrolyte solution can be characterized by studying its variation with temperature, pressure, and concentration to derive structural information related to solvent-solvent, ion-solvent, and ion-ion interactions. The existence of different ionic species such as hydrated ions and solvent-separated, solvent-shared, and contact ion pairs in an electrolyte solution can be deduced from transport properties and isentropic compressibility in conjunction with the Raman spectra. The presence of these ionic species in different concentration regions causes a transition in the physicochemical properties and their influence on the transport properties has not been studied systematically. Therefore, in this paper, the speed of sound, viscosity, and Raman spectra of $Ca(NO_3)_2$(aq) and $Cd(NO_3)_2$(aq) solutions are reported as functions of molality and temperature.

2. EXPERIMENTAL

LR grade $Ca(NO_3)_2{\cdot}4H_2O$(s) and $Cd(NO_3)_2{\cdot}4H_2O$(s) (>98%, E. Merck, India) were recrystallized twice from double-distilled water and kept in a vacuum desiccator over P_2O_5. The salts were further dried to their anhydrous state by heating them at 150°C under vacuum. Double-distilled water was used to prepare the aqueous solutions. All solutions were prepared by mass with ±0.1% uncertainty and the molality of all solutions was finally checked by EDTA titration for Ca^{2+} and gravimetrically for Cd^{2+}.

Measurements of the speed of sound at 2 MHz, the density and the recording of Raman spectra were carried out as described elsewhere.[34] The uncertainties for the measured speed of sound and density are ±0.1 m-s^{-1} and ±0.01%, respectively. The Raman spectra were recorded at room temperature with a wave number accuracy of 2 cm^{-1}.

Viscosity measurements of all solutions were performed using a Schott-Geräte AVS 310 unit equipped with a Ubbelohde viscometer. Viscometers having different cell constants (0.009595, 0.03004, and 0.1126 mm^2-s^{-2}) were used to measure the efflux times in different molality ranges. The experimental uncertainty for the viscosities of all solutions was less than ±0.4%.

The measurements were done as functions of molality ($0.0124 \leq m/(\text{mol-kg}^{-1}) \leq 12.26$ for $Ca(NO_3)_2$(aq) and $0.1668 \leq m/(\text{mol-kg}^{-1}) \leq 14.08$ for $Cd(NO_3)_2$(aq) solutions, respectively) and temperature ($273.15 \leq T/\text{K} \leq 323.15$).

3. RESULTS AND DISCUSSION

The measured density (ρ) values of $Ca(NO_3)_2$(aq) and $Cd(NO_3)_2$(aq) solutions are summarized in Table SI (Supporting Information) and the values of the parameters of the density equation, $\rho = a - b(T - 273.15)$, are given in Table I.

Table I. Least-Squares Fitted Parameters of the Density Equation, $\rho = a - b(T - 273.15)$ for $Ca(NO_3)_2$(aq) and $Cd(NO_3)_2$(aq) Solutions

m (mol-kg^{-1})	a (kg-m^{-3})	b (kg-m^{-3}-K^{-1})	σ^a in ρ (kg-m^{-3})
	Aqueous calcium nitrate		
0.0124	1010.8 ± 1.0	0.4831 ± 0.0289	0.3
0.1106	1022.6 ± 0.2	0.4002 ± 0.0062	0.1
0.4090	1062.0 ± 0.6	0.4713 ± 0.0143	0.2
0.8754	1115.5 ± 0.6	0.4939 ± 0.0151	0.3
1.511	1179.9 ± 0.5	0.5819 ± 0.0114	0.2
2.211	1241.5 ± 0.4	0.6132 ± 0.0109	0.2
2.703	1289.3 ± 0.5	0.7189 ± 0.0111	0.2
3.037	1307.9 ± 0.3	0.6735 ± 0.0090	0.1
3.635	1355.7 ± 0.2	0.6532 ± 0.0048	0.1
4.612	1423.9 ± 0.6	0.7896 ± 0.0160	0.3
5.782	1486.6 ± 0.5	0.8162 ± 0.0132	0.2
6.400	1516.0 ± 0.2	0.7935 ± 0.0065	0.1
6.895	1541.4 ± 0.6	0.8483 ± 0.0167	0.4
7.548	1576.2 ± 0.5	0.8789 ± 0.0129	0.2
8.769	1621.1 ± 0.6	0.9044 ± 0.0142	0.3
9.052	1631.4 ± 0.5	0.9019 ± 0.0135	0.3
10.05	1665.8 ± 0.5	0.9002 ± 0.0137	0.3
10.82	1697.8 ± 0.8	0.9312 ± 0.0187	0.3
12.26	1725.5 ± 0.7	0.8641 ± 0.0160	0.4
	Aqueous cadmium nitrate		
0.1668	1040.2 ± 0.2	0.4261 ± 0.0040	0.1
0.4818	1097.3 ± 0.5	0.4621 ± 0.0123	0.2
1.004	1190.0 ± 0.4	0.5544 ± 0.0117	0.3
1.491	1270.9 ± 0.4	0.6266 ± 0.0107	0.2
1.997	1349.1 ± 0.4	0.6646 ± 0.0109	0.2
2.392	1406.8 ± 0.7	0.7594 ± 0.0158	0.3
3.052	1499.7 ± 0.1	0.8299 ± 0.0009	0.1
3.100	1506.3 ± 0.9	0.8141 ± 0.0220	0.3
3.502	1553.1 ± 0.5	0.8054 ± 0.0123	0.3
3.994	1612.2 ± 0.6	0.8552 ± 0.0150	0.3
5.002	1721.1 ± 0.5	0.8620 ± 0.0122	0.3
6.654	1877.4 ± 0.7	0.9777 ± 0.0172	0.4
7.940	1982.3 ± 0.6	1.0920 ± 0.0160	0.3
10.03	2125.3 ± 0.7	1.1840 ± 0.0190	0.4
11.78	2220.4 ± 0.7	1.2440 ± 0.0170	0.3
14.08	2329.3 ± 0.9	1.3050 ± 0.0210	0.3

[a] σ denotes the standard deviation.

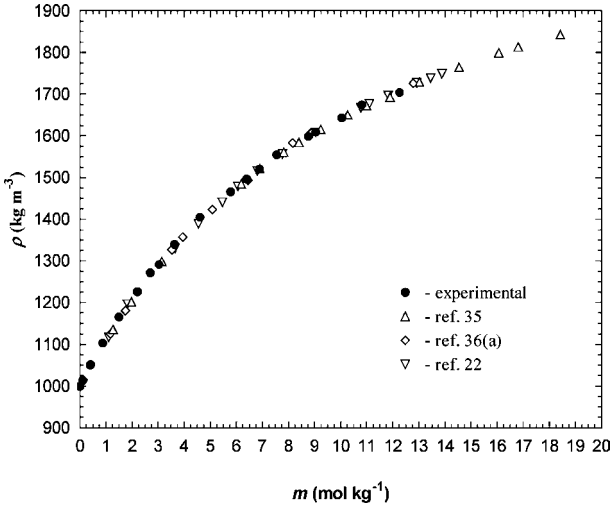

Fig. 1. Plot of the density isotherm of $Ca(NO_3)_2$(aq) solutions at 298.15 K along with the literature values.

As an example, the density isotherms of $Ca(NO_3)_2$(aq) and $Cd(NO_3)_2$(aq) are illustrated in Figs. 1 and 2, respectively, along with the reported values. The measured density values for $Ca(NO_3)_2$(aq) solutions are comparable within $\pm 0.5\%$ with the literature values.[22,35,36a] In the case of $Cd(NO_3)_2$(aq) solutions the

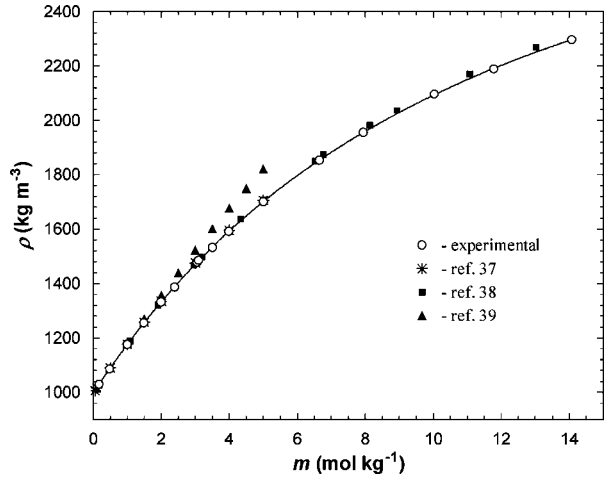

Fig. 2. Plot of the density isotherm of aqueous $Cd(NO_3)_2$(aq) solutions at 298.15 K along with the literature values.

deviations remain within ±0.3% compared with the density data reported in the literature.[37,38] However, when compared with the values of Doan and Sangster,[39] the present density values are in good agreement, within ±0.5% up to 1.0 mol-kg^{-1}, but beyond 1.0 mol-kg^{-1} the deviations increase up to ≈7.0% (Fig. 2).

The measured values of the speed of sound (u) in $Ca(NO_3)_2$(aq) and $Cd(NO_3)_2$(aq) solutions are presented in Table SII (Supporting Information) as functions of molality and temperature. The experimental speed of sound values in $Ca(NO_3)_2$(aq) and $Cd(NO_3)_2$(aq) solutions are in agreement within ±0.6 and 0.1% with the values of Carpio *et al.*[22] and Jha and Jha[40] at 298.15 and 296.15 K, respectively.

The experimental viscosity (η) values for $Ca(NO_3)_2$(aq) and $Cd(NO_3)_2$(aq) solutions are presented in Table SIII (Supporting Information) at various molalities and temperatures. For $Ca(NO_3)_2$(aq) solutions, the viscosity values agree within ±1.9% up to 6.4 mol-kg^{-1} with the values of Mahiuddin and Ismail,[36a] but the deviations increase to ±6.5% at higher molalities. Whereas, the viscosities for $Cd(NO_3)_2$(aq) solutions are comparable within ±4.5% with the values of Isono.[37] The viscosity values of Doan and Sangster[39] are in good agreement, within ±5% up to 2 mol-kg^{-1}, with the present results as well as those of Isono.[37]

3.1. Isentropic Compressibility

Before dealing with the isentropic compressibility isotherms, we plotted $(u - u_0)/m$ *versus* $\sqrt{m}$ for both the systems at 298.15 K, see Fig. 3. It is interesting

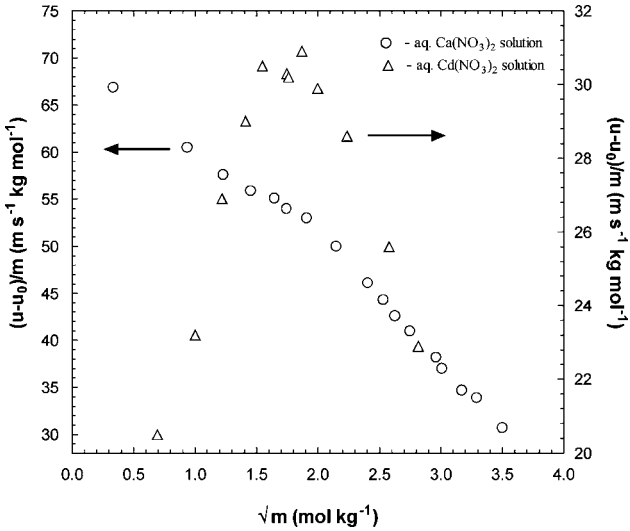

Fig. 3. Plots of $(u - u_0)/m$ *versus* $\sqrt{m}$ for $Ca(NO_3)_2$(aq) and $Cd(NO_3)_2$(aq) solutions at 298.15 K.

to note that the variation of $(u - u_0)/m$ with $\sqrt{m}$ up to certain molalities for both the systems are opposite in nature, and the plots show a transition over a narrow molality region. A similar transition in $(u - u_0)/m$ *versus* $\sqrt{m}$ plot, as in the case of $Ca(NO_3)_2$(aq) solutions, has been reported for several aqueous chloride salt solutions and this transition has been correlated with the hydration structure around cations and anions of the systems.[41] In $Ca(NO_3)_2$(aq) and $Cd(NO_3)_2$(aq) such a transition occurs at ≈3.4 and 3.8 mol-kg^{-1}, respectively.

The phase diagrams constructed, not shown here, from literature data[38,42] for $Ca(NO_3)_2$(aq) and $Cd(NO_3)_2$(aq) exhibit a structural transition due to the first eutectic point at ≈4.6 and 2.4 mol-kg^{-1} corresponding to $[Ca(NO_3)_2 \cdot 12H_2O]$ and $[Cd(NO_3)_2 \cdot 23H_2O]$, respectively. The variation of $(u - u_0)/m$ with $\sqrt{m}$ (Fig. 3), and the phase diagram for both aqueous systems, imply that the structural transition occurs gradually over a narrow molality region. Considering the primary hydration number of Cd^{2+}, Ca^{2+}, and NO_3^- as being 8, 6, and 6, respectively,[5,13] the Cd^{2+} and NO_3^-, and Ca^{2+}, and NO_3^- systems in water require 20 and 18 molecules of water to complete their respective primary hydration spheres, which correspond to ≈2.8 and 3.1 mol-kg^{-1}, respectively. Thus, the molality at which transition in the $(u - u_0)/m$ *versus* $\sqrt{m}$ plot occurs can be viewed as that for the transition from free hydrated ions to solvent-separated and/or solvent-shared ion-pairs.

The isentropic compressibilities (κ_s) of the present systems were calculated using the following equation

$$\kappa_s = (u^2 \rho)^{-1} \tag{1}$$

The κ_s *versus m* isotherms for $Ca(NO_3)_2$(aq) and $Cd(NO_3)_2$(aq) solutions at three temperatures are illustrated in Figs. 4 and 5, respectively.

An empirical equation[43] that has been used to represent the molality dependence of the isentropic compressibilities is

$$\kappa_s = a_1 + b_1 m + c_1 m^{1.5} + d_1 m^2 + e_1 m^{2.5} + f_1 m^3 \tag{2}$$

In Eq. (2), a_1, b_1, c_1, d_1, e_1, and f_1 are temperature-dependent parameters and m is the molality in mol-kg^{-1}. The estimated values of the parameters of Eq. (2) are listed in Table II.

A comparison of the isentropic compressibility isotherms of the present systems at 298.15 K is depicted in Fig. 6. This plot shows that $Cd(NO_3)_2$(aq) is less compressible in comparison to $Ca(NO_3)_2$(aq) at a fixed molality. The X-ray diffraction studies showed that the $Cd^{2+}—OH_2$ and $Ca^{2+}—OH_2$ bond distances due to cation hydration are 228 pm and 247 pm, respectively.[1,5,44] The $Ca^{2+}—OH_2$ bond distance is longer in comparison to $Cd^{2+}—OH_2$, thereby, the isentropic compressibility of a $Ca(NO_3)_2$(aq) solution is also larger. To support this view, we have included the isentropic compressibility isotherm of $Zn(NO_3)_2$(aq)[45] at 298.15 K in Fig. 6. The $Zn^{2+}—OH_2$ bond distance is 217 pm,[46] so the isentropic

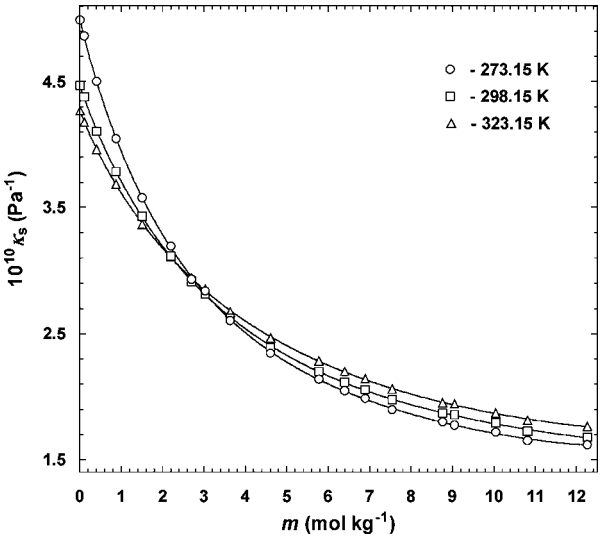

Fig. 4. Variation of the isentropic compressibility (κ_s) with molality (m) at three temperatures for $Ca(NO_3)_2$(aq) solutions (symbols and solid curves represent the experimental and calculated [from Eq. (2)] values, respectively).

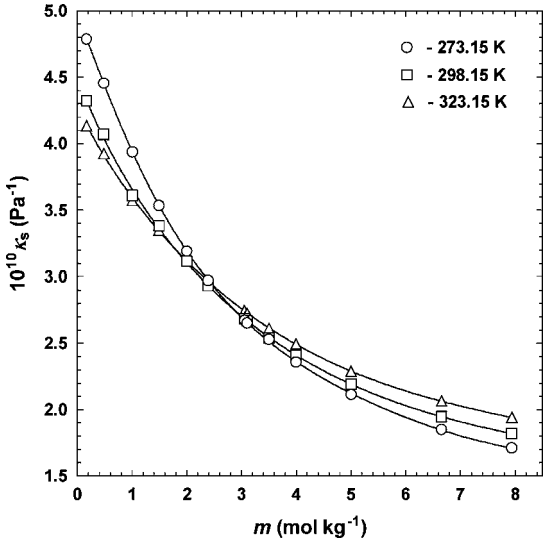

Fig. 5. Variation of the isentropic compressibility (κ_s) *versus* molality (m) at three temperatures for $Cd(NO_3)_2$(aq) solutions (symbols and solid curves represent the experimental and calculated [from Eq. (2)] values, respectively).

Table II. Values of the Parameters of Eq. (2) for $Ca(NO_3)_2$(aq) and $Cd(NO_3)_2$(aq) Solutions

Parameters	273.15 K	298.15 K	323.15 K
	Aqueous calcium nitrate		
$10^{10}a_1$ (Pa^{-1})	5.0108 ± 0.0109	4.4796 ± 0.0084	4.2755 ± 0.0074
$10^{10}b_1$ (Pa^{-1}-kg-mol^{-1})	-1.5794 ± 0.1025	-1.0965 ± 0.0786	-0.9720 ± 0.0692
$10^{10}c_1$ (Pa^{-1}-$kg^{1.5}$-$mol^{-1.5}$)	0.4945 ± 0.1679	0.3111 ± 0.1288	0.3360 ± 0.1134
$10^{10}d_1$ (Pa^{-1}-kg^2-mol^{-2})	0.0680 ± 0.1044	0.0366 ± 0.0801	-0.0149 ± 0.0705
$10^{10}e_1$ (Pa^{-1}-$kg^{2.5}$-$mol^{-2.5}$)	-0.0504 ± 0.0285	-0.0250 ± 0.0218	-0.0102 ± 0.0192
$10^{12}f_1$ (Pa^{-1}-kg^3-mol^{-3})	0.5985 ± 0.2856	0.2680 ± 0.2192	0.1410 ± 0.1930
$10^{12}\sigma$ (Pa^{-1})	1.24	0.95	0.84
	Aqueous cadmium nitrate		
$10^{10}a_1$ (Pa^{-1})	4.9427 ± 0.0228	4.5174 ± 0.0611	4.2828 ± 0.0281
$10^{10}b_1$ (Pa^{-1}-kg-mol^{-1})	-0.5014 ± 0.2329	-1.3561 ± 0.6270	-0.9907 ± 0.2884
$10^{10}c_1$ (Pa^{-1}-$kg^{1.5}$-$mol^{-1.5}$)	-1.5514 ± 0.4357	0.6138 ± 1.1678	0.3589 ± 0.5372
$10^{10}d_1$ (Pa^{-1}-kg^2-mol^{-2})	1.4699 ± 0.3167	-0.1431 ± 0.8488	-0.0762 ± 0.3905
$10^{10}e_1$ (Pa^{-1}-$kg^{2.5}$-$mol^{-2.5}$)	-0.4705 ± 0.1025	0.0287 ± 0.2748	0.0242 ± 0.1264
$10^{12}f_1$ (Pa^{-1}-kg^3-mol^{-3})	5.268 ± 1.232	-0.3470 ± 3.302	-0.3985 ± 1.519
$10^{12}\sigma$ (Pa^{-1})	0.83	2.22	1.02

compressibility should be in the order of $Ca(NO_3)_2 > Cd(NO_3)_2 > Zn(NO_3)_2$, and this trend is observed in this plots (Fig. 6).

Figures 4 and 5 show that the isentropic compressibility decreases with an increase in salt content because of the simultaneous effects of hydration of ions

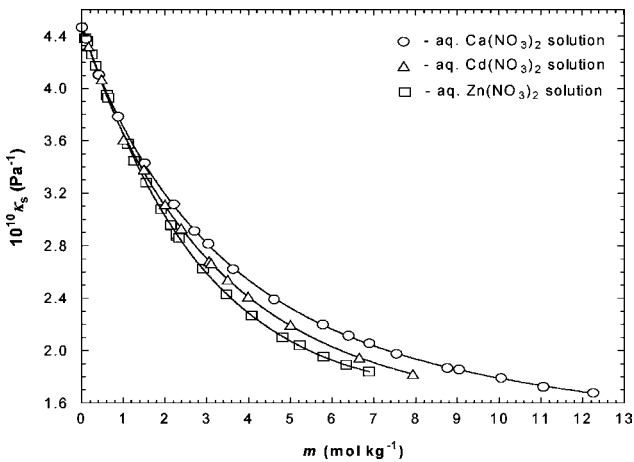

Fig. 6. Comparison of the isentropic compressibility isotherms (κ_s) for $Ca(NO_3)_2$(aq), $Cd(NO_3)_2$(aq), and $Zn(NO_3)_2$(aq) solutions at 298.15 K (symbols and solid curves represent the experimental and calculated [from Eq. (2)] values, respectively).

and breaking of the network structure of water. The κ_s *versus* m isotherms (Figs. 4 and 5) converge or cross over a narrow molality region, due to the complete breaking up of the inherent water structure and completion in the primary hydration shell of ions. The isentropic compressibility of aqueous electrolyte solutions is due to about 64% configurational and 36% vibrational compressibility.[47] In dilute solutions the isentropic compressibility is predominantly governed by the configurational part, whereas in concentrated solutions it is due predominantly to the vibrational part. Thus, from the behavior of isentropic compressibility isotherms (Figs. 4 and 6), one can conclude that isentropic compressibility is the sum of two contributions: $\kappa_{s(\text{solvent intrinsic})}$ and $\kappa_{s(\text{solute intrinsic})}$. $\kappa_{s(\text{solvent intrinsic})}$ is the isentropic compressibility due to the compression of the three dimensional network structure of water and $\kappa_{s(\text{solute intrinsic})}$ is the isentropic compressibility due to the compression of the hydration shell of the ions.

It appears that the temperature derivative of κ_s is more informative. The following equation

$$\kappa_s = a_2 + b_2 T + c_2 T^2 \tag{3}$$

can adequately describe the temperature dependence of the isentropic compressibility. In Eq. (3), a_2, b_2, and c_2 are adjustable parameters and T is the absolute temperature. The temperature derivatives of κ_s for both $Ca(NO_3)_2$(aq) and $Cd(NO_3)_2$(aq) solutions at 298.15 K are shown in Fig. 7. It is apparent that $(d\kappa_s/dT)$ becomes zero at $\approx$2.72 and 2.48 mol-kg^{-1} for $Ca(NO_3)_2$(aq) and $Cd(NO_3)_2$(aq) solutions, respectively within the temperature range of the study. These zero derivative values imply that the ionic species or complexes formed at these particular molalities of the respective systems are thermodynamically stable and result

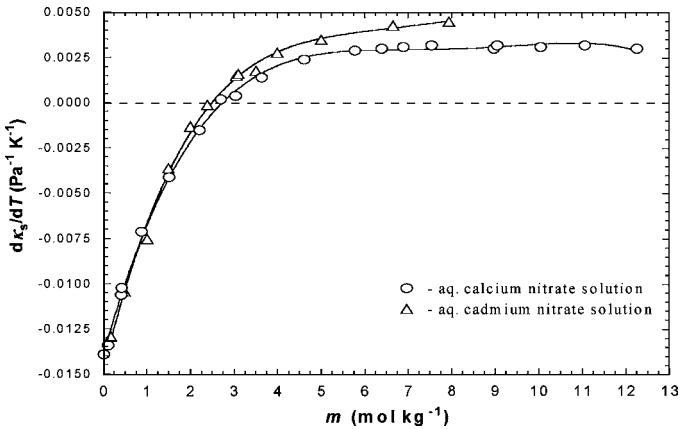

Fig. 7. Plots of $(d\kappa_s/dT)$ *versus* molality (m) for aqueous $Ca(NO_3)_2$(aq) and $Cd(NO_3)_2$(aq) solutions at 298.15 K.

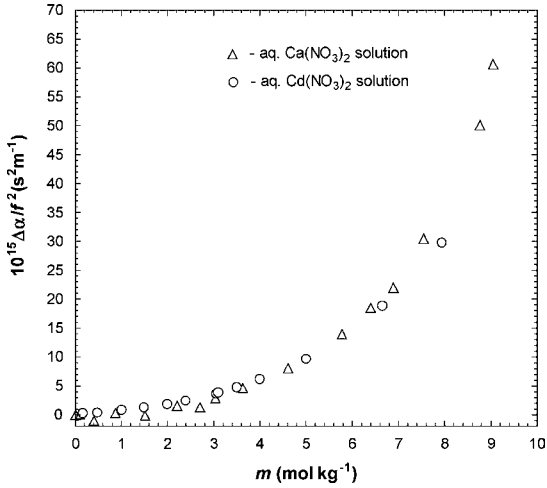

Fig. 8. Plot of $(\Delta\alpha/f^2)_{cl}$ *versus* molality (m) of $Ca(NO_3)_2$(aq) and $Cd(NO_3)_2$(aq) solutions at 298.15 K.

in rigid structures as all the water molecules reside in the primary hydration shell of the ions.

Endo and Nomoto[48] observed that the sound absorption reaches a minimum value at a particular molality when all of the water molecules are contained in the primary hydration shell of the electrolyte. Therefore, the classical sound absorption differences, $(\Delta\alpha/f^2)_{\rm cl}$, between the solution and solvent for both the systems were calculated using the following equation[48]

$$(\Delta a/f^2)_{\rm c1} = (8\pi^2/3)\left(\eta/\rho u^3 - \eta_0/\rho_0 u_0^3\right) \tag{4}$$

where ρ, u, η, ρ_0, u_0, and η_0 are the density, speed of sound, and viscosity of the solution and solvent, respectively. The variation of $(\Delta\alpha/f^2)_{\rm cl}$ with molality for aqueous $Ca(NO_3)_2$(aq) and $Cd(NO_3)_2$(aq) solutions are plotted in Fig. 8 at 298.15 K. In the present systems, unlike the minimum observed in the $(\Delta\alpha/f^2)_{\rm cl}$ *versus* m plot, $(\Delta\alpha/f^2)_{\rm cl}$ varies linearly with molality up to $\approx$2.5 mol-kg^{-1}, which corresponds to the concentration at which the κ_s isotherms (Figs. 4 and 5) cross over for both of the systems.

3.2. Shear Relaxation Time

The shear relaxation time (τ) of $Ca(NO_3)_2$(aq) and $Cd(NO_3)_2$(aq) solutions were calculated using the following relation

$$\tau = 4\eta/3u^2\rho \tag{5}$$

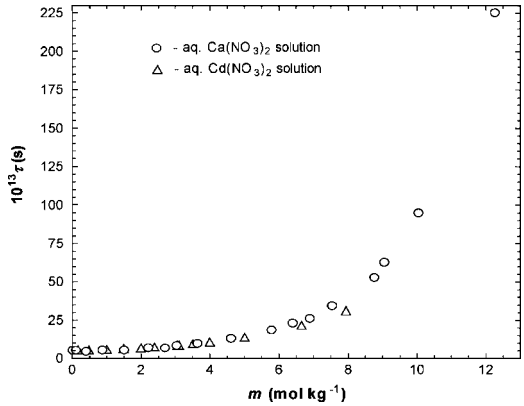

Fig. 9. Variation of the shear relaxation time (τ) with molality (m) of aqueous $Ca(NO_3)_2$(aq) and $Cd(NO_3)_2$(aq) solutions at 298.15 K.

The τ *versus* m plots for $Ca(NO_3)_2$(aq) and $Cd(NO_3)_2$(aq) solutions at 298.15 K are depicted in Fig. 9. In $Ca(NO_3)_2$(aq) and $Cd(NO_3)_2$(aq) solutions, the τ values are almost independent of molality up to $\approx$2–3 mol-kg^{-1} where the coupling force resulting from ion-solvent interactions governs the τ values. Beyond $\approx$2–3 mol-kg^{-1}, the τ values increase exponentially with molality where ion pairing occurs extensively. At higher temperatures, the τ *versus* m curves are more or less monotonous. However, as the temperature is decreased, the τ *versus* m plots become more and more exponential. This trend in the τ *values*, which incorporates shear effects, prevails because both hydrogen bonds in anion hydration and in water are reinforced[1,49] at low temperatures, which favors the formation of contact ion pairing.[1] As the NO_3^- is large compared to the cations, it can be concluded that anion progressively controls the shear effects in both systems.

The most striking feature of concentrated electrolyte solutions is that, at a particular molality, the electrical conductivity (κ) reaches a maximum. Claes *et al.*[50] suggested that at that concentration the primary hydration of the solute becomes complete. For this case, the ions should form a stable and rigid structure, so an electrolyte solution will exhibit a maximum conductivity with an insignificant change in relaxation time. A good correspondence of different concentration regions can be inferred from the plots of κ *versus* τ. Therefore, plots of reported electrical conductivity[36b,37] *versus* τ for both the systems are illustrated in Fig. 10.

For both the systems, the electrical conductivity increases sharply and the maximum conductivity is observed at $\tau \approx 7 \times 10^{-13}$ s, which corresponds to $\approx$1.99 mol-kg^{-1} for both the systems. This fact implies that up to $\approx$1.99 mol-kg^{-1}, both unassociated and hydrated ions are present. Above $\approx$1.99 mol-kg^{-1} the electrical conductivity decreases monotonically with the increase in relaxation

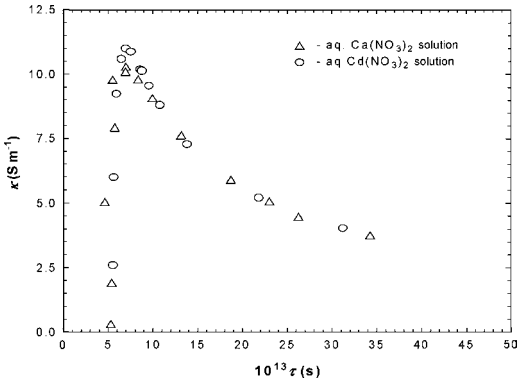

Fig. 10. Variation of the electrical conductivity (κ) with shear relaxation time (τ) at 298.15 K for $Ca(NO_3)_2$(aq) and $Cd(NO_3)_2$(aq) solutions.

time, because the number of water molecules per ion decreases with the increase in molality and NO_3^- enters into the hydration shell of the calcium and cadmium ions, forming solvent-separated and/or solvent-shared ion pairs. Up to $\approx$1.99 mol-kg^{-1} the number of water molecules present in the secondary hydration sphere gradually decreases and as a result the size of the migrating entity decreases and the mobility increases with almost constant shear relaxation time for both systems.

3.3. Raman Spectra

The Raman spectra in the frequency range of 200 to 1600 cm^{-1} of $Ca(NO_3)_2$(aq) and $Cd(NO_3)_2$(aq) solutions in the molality ranges 0.5292 to 7.415 mol-kg^{-1} and 0.4643 to 7.794 mol-kg^{-1}, respectively, are depicted in Figs. 11 and 12. The frequencies of the nitrate modes and the libration band (ν_{lib}) of water are tabulated in Table III. There are remarkable changes in the modes at 346 and 715 cm^{-1} and in the spectral envelope at $\approx$1400 cm^{-1}, corresponding to the $\nu(M^{n+}—OH_2)$ mode, and in the ν_4 and ν_3 modes of NO_3^-, respectively. The band at 1047 cm^{-1} does not shift for the $Cd(NO_3)_2$(aq) solutions, but in $Ca(NO_3)_2$(aq) solutions it shifts $\approx$3 cm^{-1} to higher frequency, which implies that the NO_3^- is unbound with D_{3h} symmetry in $Cd(NO_3)_2$(aq) solution.

It is interesting to note that the band at $\approx$346 cm^{-1} in the case of the 0.4643 mol-kg^{-1} $Cd(NO_3)_2$(aq) solution is assigned to the symmetric stretching mode of $\nu(Cd^{2+}—OH_2)$.[51,52] As the molality increases, the band at 346 cm^{-1} is shifted to lower frequency with increasing intensity and is centered at 333 cm^{-1}. Spohn and Brill[18] reported a similar shift of the libration band, which corresponds to the $\nu_{(Cd^{2+}-OH_2)}$ mode, to a lower frequency and a decreasing intensity with increasing temperature. Also, the D_{3h} symmetry of the "hydrated NO_3^-" or "free"

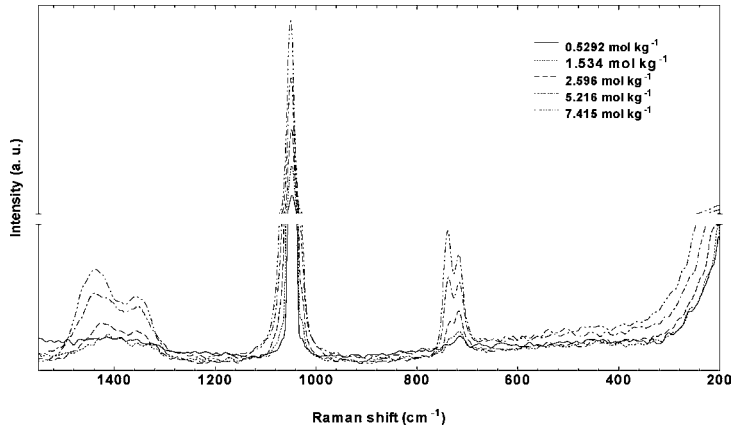

Fig. 11. Raman spectra of $Ca(NO_3)_2$(aq) solutions at various molalities.

NO_3^- is perturbed as the molality is increased, causing shifts of the $\nu_{(Cd^{2+}-OH_2)}$ mode. Unlike the $Cd(NO_3)_2$(aq) solutions, no band corresponding to $\nu_{(Cd^{2+}-OH_2)}$ is detected, due to the flexible hydration behavior of Ca^{2+}.

The spectral features of NO_3^- in the 700 cm^{-1} region (ν_4 mode) are generally taken as evidence for ion-pair formation.[18,24,30,32,53] The NO_3^- with D_{3h} symmetry exhibits a band at ≈715 cm^{-1} in solutions (≈0.5 mol-kg^{-1}) of $Ca(NO_3)_2$(aq) and $Cd(NO_3)_2$(aq) (Figs. 11 and 12). This result implies that at this molality the hydrated NO_3^- ion is unbound. As the molality increases to ≈1.5 mol-kg^{-1}, a weak shoulder appears at 733 cm^{-1} in $Ca(NO_3)_2$(aq) solutions (Fig. 11), but no corresponding band at ≈733 cm^{-1} is detected for $Cd(NO_3)_2$(aq) solution at

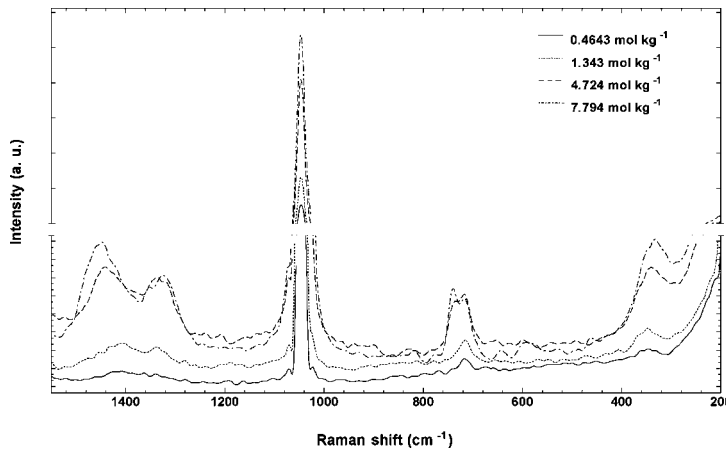

Fig. 12. Raman spectra of $Cd(NO_3)_2$(aq) solutions at various molalities.

Table III. Band Parameters Corresponding to the Nitrate Modes and the Libration (ν_{lib}) of Water for $Ca(NO_3)_2$(aq) and $Cd(NO_3)_2$(aq) Solutions at Room Temperature

	Peak position[a] (cm^{-1})					
	Mode					
Concentration (mol-kg^{-1})	ν_{lib}	ν_1		ν_3		ν_4
		Aqueous calcium nitrate				
0.5292		1047 (vs)		1415 (bw)	715 (m)	
1.534		1048 (vs)	1355 (w)	1412 (m)	716 (m)	733 (w)
2.534		1049 (vs)	1356 (m)	1426 (m)	717 (m)	734 (m)
5.216		1049 (vs)	1353 (m)	1439 (s)	716 (m)	738 (s)
7.415		1050 (vs)	1357 (m)	1437 (s)	717 (m)	739 (s)
		Aqueous cadmium nitrate				
0.4643	346 (w)	1047 (vs)		1406 (bw)	717 (m)	
1.343	348 (m)	1047 (vs)	1338 (m)	1406 (m)	716 (m)	
4.724	340 (s)	1047 (vs)	1336 (s)	1442 (s)	717 (m)	737 (m)
7.794	333 (s)	1047 (vs)	1324 (s)	1447 (s)	717 (m)	740 (s)

[a] bw, broad weak; m, medium; s, sharp; vs, very sharp.

corresponding molalities. Upon further increasing the molality, the intensity of the band at $\approx$733 cm^{-1} gradually increases and shifts $\approx$6 cm^{-1} to the higher frequency, but the intensity of the $\approx$715 cm^{-1} mode gradually decreases as the molality increases. Similar spectral changes with the increases in molality for $Cd(NO_3)_2$(aq) and $Ca(NO_3)_2$(aq) have been reported in the literature.[25,32,51,52] In $Cd(NO_3)_2$(s), the 715 cm^{-1} mode vanishes and the band at 740 cm^{-1} becomes intense,[32] suggesting that the NO_3^- is bound directly and stoichiometrically to Cd^{2+}.

The results imply that up to $\approx$0.5 mol-kg^{-1} the NO_3^- ion is fully hydrated and unbound. As the molality increases above this value, the NO_3^- enters the hydration sphere of the cation and forms solvent-separated and/or solvent shared ion pairs within the molality range of this study.

The spectral change for the ν_3 mode ($\approx$1400 cm^{-1}) for both systems is also taken as an indicator for the presence of complex or ion-pair formation in many nitrate salts solutions.[18,25,53,54] Raman spectra (Figs. 11 and 12) show that for dilute solutions (up to $\approx$0.5 mol-kg^{-1}), a weak spectral envelope appears at $\approx$1410 cm^{-1} for both aqueous systems investigated. With an increase in molality, the ν_3 asymmetric mode produces an additional component at 1338 and 1355 cm^{-1}, for 1.534 and 1.343 mol-kg^{-1} $Ca(NO_3)_2$(aq) and $Cd(NO_3)_2$(aq) solutions, respectively. As the molality further increases, unlike the ν_4 mode, the intensites of the two bands of the ν_3 mode increase and $\Delta\nu$ is enhanced. For $Cd(NO_3)_2$(aq) and $Ca(NO_3)_2$(aq) solutions at 7.794 and 7.415 mol-kg^{-1}, the values of $\Delta\nu$ are 123 and 80 cm^{-1}, respectively, as a result of the perturbation of the symmetry of NO_3^- from D_{3h} to C_{2v}, and this effect is stronger in $Cd(NO_3)_2$(aq) solutions than that in $Ca(NO_3)_2$(aq) solutions. In contrast to $Ca(NO_3)_2$(aq) solution, the temperature dependence of the ν_3 asymmetric modes for $Cd(NO_3)_2$(aq) solutions

(at 4.12 mol-kg^{-1}) enhances the $\Delta\nu = 163$ cm^{-1}, although the relative intensity is unaltered in the temperature range from 26 to 375°C.[18] However, in the present study the molality dependencies of the ν_3 asymmetric modes increase the intensity of both bands and the separation is larger in $Cd(NO_3)_2$(aq) solutions, which is accounted for the higher charge to radius ratio for Cd^{2+} in comparison to Ca^{2+}.

As to the results associated with the spectral change in the ν_3 and ν_4 modes in the molalitity range of the study, the unperturbed and hydrated NO_3^- undergoes a change in symmetry from D_{3h} to C_{2v} due to its association with the Cd^{2+} and Ca^{2+}. As a result, either solvent-separated or solvent-shared ion pairs or both, *e.g.*, $[Ca^{2+}—(H_2O)_x—NO_3^-]$[12,25] and $[Cd^{2+}—(H_2O)_x—NO_3^-]$,[26,32,33] are formed in $Ca(NO_3)_2$(aq) and $Cd(NO_3)_2$(aq) solutions, which are not distinguishable by their Raman spectra. From the spectra (Figs. 11 and 12) it is apparent that the intensity of the bands at 717 and 740 cm^{-1} of the ν_4 mode for ≈4.1 mol-kg^{-1} $Ca(NO_3)_2$(aq) and 4.7 mol-kg^{-1} $Cd(NO_3)_2$(aq) solutions are almost equal, due to the coexistence of equal proportions of unbound NO_3^- with D_{3h} symmetry and bound NO_3^- with C_{2v} symmetry. Similarly, from the Raman spectra of dilute $Ca(NO_3)_2$(aq) solution (0.5 mol-dm^{-3}),[25] Fleissner *et al.*[54] suggested the presence of ≈20% bound and ≈80% "free" nitrate.

4. CONCLUSIONS

From the present investigation it is envisaged that the formation of solvent-separated and/or solvent-shared ion pairs in $Ca(NO_3)_2$(aq) and $Cd(NO_3)_2$(aq) solutions is not sudden and is not restricted to a particular molality. As a result, the isentropic compressibility isotherms do not exhibit convergence at a particular molality but rather over a narrow molality range (Figs. 4 and 5). The large $\Delta\nu$ of the ν_3 mode for $Cd(NO_3)_2$(aq) solution results from the formation of strong solvent-separated and/or solvent-shared ion pairs. Therefore, the isentropic compressibility of $Cd(NO_3)_2$(aq) solutions is less than $Ca(NO_3)_2$(aq) (Fig. 6). Even though unbound and hydrated NO_3^-, and the solvent-shared and/or solvent-separated ion pairs co-exist in dilute solution,[51] the influence of the solvent-separated and/or solvent-shared ion pairs begins ≈2 mol-kg^{-1} for both the solutions as evidenced from the κ *versus* τ plots (Fig. 10). Therefore, the results show that the presence of different ionic species in different concentration regions govern the transport properties.

ACKNOWLEDGMENTS

The authors are thankful to the Director of the laboratory for the facilities and interest in this work. NR and AW are grateful to the Council of Scientific & Industrial Research, New Delhi, India for the award of a senior research fellowship. The authors are also thankful to the Indian Association for the Cultivation of Science, Kolkata, India, for recording the Raman Spectra.

REFERENCES

1. P. Smirnov, M. Yamagami, H. Wakita, and T. Yamaguchi, *J. Mol. Liq.* **73/74**, 305 (1997) and references therein.
2. S. Cummings, J. E. Enderby, and R. A. Howe, *J. Phys. C.: Solid State Phys.* **13**, 1 (1980) and references therein.
3. S. Ansell and G. W. Neilson, *J. Chem. Phys.* **112**, 3942 (2000) and references therein.
4. M. Imano, Y. Kameda, T. Usuki, and O. Uemura, *J. Phys. Soc. Jpn.* (Suppl.) **70**, 368 (2001).
5. F. Jalilehvand, D. Spängberg, P. Lindqvist-Reis, K. Harmansson, I. Persson, and M. Sandström, *J. Am. Chem. Soc.* **123**, 431 (2001) and references therein.
6. M. I. Bernal-Uruchurtu and I. Ortega-Blake, *J. Chem. Phys.* **103**, 1588 (1995).
7. D. Spängberg, K. Hermansson, P. Lindqvist-Reis, F. Jalilehvand, M. Sandström, and I. Persson, *J. Phys. Chem. B* **104**, 10467 (2000).
8. C. F. Schwenk, H. H. Loeffler, and B. M. Rode, *Chem. Phys. Lett.* **349**, 99 (2001).
9. G. Palinkas and H. Heizinger, *Chem. Phys. Lett.* **126**, 251 (1986).
10. A. K. Katz, J. P. Glusker, S. A. Beebe, and C. W. Bock, *J. Am. Chem. Soc.* **118**, 5752 (1996).
11. W. W. Rudolph and C. C. Pye, *J. Phys. Chem. B* **102**, 3564 (1998).
12. M. Pavlov, P. E. M. Siegbahn, and M. Sandstrom, *J. Phys. Chem. A* **102**, 219 (1998).
13. H. Ohtaki and T. Radnai, *Chem. Rev.* **93**, 1157 (1993).
14. D. A. T. Dick, in *Water and Aqueous Solutions*, R. A. Horne, ed. (Wiley Interscience, New York, 1972), Chapter 7.
15. J. J. R. Frausto da Silva and R. P. J. Willimas, *The Biological Chemistry of the Elements*, (Clarendon, Oxford, 1991), Chapter 10.
16. S. A. Newman, *Thermodynamics of Aqueous Systems with Industrial Application, ACS Symposium Series 133*, (ACS, Washington DC, 1980); S. I. Smedley, *The Interpretation of Ionic Conductivity in Liquids* (Plenum Press, New York, 1980), Chapter 6.
17. D. W. James, R. F. Armishaw, and R. L. Frost, *Aust. J. Chem.* **31**, 1401 (1978).
18. P. D. Sophn and T. B. Brill, *J. Phys. Chem.* **93**, 6224 (1989).
19. A. H. Valeev, V. V. Kuznetsov, V. N. Trostin, and G. A. Krestov, *Russ. J. Inorg. Chem.* **35**, 154 (1990).
20. N. A. Hewish, G. W. Neilson, and J. E. Enderby, *Nature* **297**, 138 (1982).
21. R. Caminiti and M. Magini, *Z. Naturforsch.* **A36**, 831 (1981).
22. R. Carpio, M. Mehicic, F. Borsay, C. Petrovic, and E. Yeager, *J. Phys. Chem.* **86**, 4980 (1982).
23. R. E. Hester and R. A. Plane, *J. Chem. Phys.* **40**, 411 (1964).
24. R. E. Hester and R. A. Plane, *Inorg. Chem.* **3**, 769 (1964).
25. D. E. Irish and G. E. Walrafen, *J. Chem. Phys.* **46**, 378 (1967).
26. D. E. Irish, A. R. Davies, and R. A. Plane, *J. Chem. Phys.* **50**, 2262 (1969).
27. D. W. James and R. L. Frost, *Aust. J. Chem.* **35**, 1793 (1982).
28. W. Bol, G. J. A. Gerrits, and C. L. Van Panthaleon van Eck, *J. Appl. Crystallogr.* **3**, 486 (1970).
29. V. V. Kuznetsov, V. N. Trostin, and G. A. Izv. Krestov, *Vyssh. Uchebn. Zavd., Khim. Kim. Tekhnol.* **25**, 954 (1982).
30. H. Kanno, *Bull. Chem. Soc. Jpn.* **59**, 3651 (1986).
31. A. Kh. Valeev, V. V. Kuznetsov, V. N. Trostin, and G. A. Krestov, *Dokl. Akad. Nauk. SSSR*, **285**, 911 (1986).
32. R. Caminiti, P. Cucca, and T. Radnai, *J. Phys. Chem.* **88**, 2382 (1984).
33. A. R. Davies and R. A. Plane, *Inorg. Chem.* **7**, 2565 (1968).
34. N. Rohman, A. Wahab, N. N. Dass, and S. Mahiuddin, *Fluid Phase Equilib.* **178**, 277 (2001); N. Rohman, N. N. Dass, and S. Mahiuddin, *J. Mol. Liquids*, **100/3**, 265 (2002).
35. W. W. Ewing and R. J. Mikovsky, *J. Am. Chem. Soc.* **72**, 1390 (1950).

36. (a) S. Mahiuddin and K. Ismail, *J. Phys. Chem.* **87**, 5241 (1983). (b) S. Mahiuddin and K. Ismail, *J. Phys. Chem.* **88**, 1027 (1984).
37. T. Isono, *J. Chem. Eng. Data* **29**, 45 (1984).
38. J. Timmermans, *The Physico-Chemical Constant of Binary Systems in Concentrated Solutions*, (Interscience Publishers, New York, 1960).
39. T. H. Doan and J. Sangster, *J. Chem. Eng. Data* **26**, 141 (1981).
40. D. K. Jha and B. L. Jha, *Ind. J. Pure Appl. Phys.* **28**, 346 (1990).
41. F. J. Millero, M. Fernandez, and E. Vinokurova, *J. Phys. Chem.* **89**, 1062 (1985).
42. C. A. Angell and E. J. Sare, *J. Chem. Phys.* **52**, 1058 (1970).
43. F. J. Millero, J. Ricco, and D. R. Schreiber, *J. Solution Chem.* **11**, 671 (1982).
44. R. Caminiti, D. Atzei, P. Cucca, A. Anedla, and G. Bongiovanni, *J. Phys. Chem.* **90**, 238 (1986).
45. A. Wahab and S. Mahiuddin, *J. Chem. Eng. Data* **49**, 126 (2004).
46. S. P. Dagnall, D. N. Hague, and A. D. C. Towl, *J. Chem. Soc. Faraday Trans. 2*, **78**, 2161 (1982).
47. W. M. Slie, A. R. Donfor, and T. A. Litovitz, *J. Chem. Phys.* **44**, 3712 (1966).
48. H. Endo and O. Nomoto, *J. Chem. Soc., Faraday Trans. 2*, **77**, 217 (1981).
49. K. Yamanaka, M. Yamagami, K. Takamuku, T. Yamaguchi, and H. Wakita, *J. Phys. Chem.* **97**, 10835 (1993).
50. P. Claes, G. Y. Liox, and J. Gilber, *Electrochim. Acta* **28**, 421 (1983).
51. M. T. Carrick, D. W. James, and W. M. Leong, *Aust. J. Chem.* **36**, 223 (1983).
52. W. W. Rudolph and C. C. Pye, *J. Phys. Chem. B* **102**, 3564 (1998).
53. G. Fleissner, A. Hallbrucker, and E. Mayer, *Chem. Phys. Lett.* **218**, 93 (1994).
54. G. Fleissner, A. Hallbrucker, and E. Mayer, *J. Phys. Chem.* **97**, 4806 (1993).